Materials Horizons

COMMUNICATION

View Article Online
View Journal

Cite this: DOI: 10.1039/c8mh00817e

Received 11th July 2018,
Accepted 17th August 2018

DOI: 10.1039/c8mh00817e

rsc.li/materials-horizons

Interlayer crosslinking to conquer the stress relaxation of graphene laminated materials†

Mincheng Yang,[a] Zhen Xu, *[ab] Peng Li,[a] Fan Guo,[a] Yingjun Liu,[a] Youhua Xiao,[a] Weiwei Gao [a] and Chao Gao *[a]

For any structural material, mechanical relaxation is a vital factor to determine its capability to bear dynamic loading. Macroscopically assembled graphene materials (MAGMs) have emerged as promising carbonaceous materials with high mechanical strength for potential structural uses. Considerable effort has been initially focused on the promotion of mechanical strength, most of it static. However, dynamic mechanical behaviour has long been ignored. Here, we observed a severe relaxation behaviour of macroscopically assembled graphene papers with laminated structures caused by the viscoelastic nature of the interlayer interactions. We found that the relaxation behaviour of laminated structures of two-dimensional graphene conforms to a ternary Maxwell–Wiechert model. The relaxation was considerably relieved by enhanced interlayer crosslinking to retard interlayer slippage. With the enhancements of crosslinking strength and increasing density, permanent stress was promoted to 84.1%, significantly higher than 14.7% for graphene oxide papers and 43.2% for the original reduced graphene papers. Analogous to chemically crosslinked polymeric rubbers, we used this interlayer crosslinking method to relieve the mechanical relaxation and improve the stretching elasticity of graphene laminated materials at a large strain of 10%. Our work reveals an ignored relaxation behaviour of MAGMs and develops an efficient interlayer crosslinking strategy to conquer stress relaxation, enabling the modulation of structures and properties under general guidance and paving the way for their realistic applications as structural materials.

Conceptual insights

Stress relaxation is a vital dynamic mechanical behaviour for any structural material. Macroscopically assembled graphene materials (MAGMs), exemplified by strong graphene papers and fibres, are no exception. However, their dynamic behaviour has long been ignored. In this communication, we uncover a severe stress relaxation problem for graphene papers. This finding can attract more attention to the dynamic mechanical behaviour of MAGMs, beyond promoting static strength. We also propose a rational Maxwell–Wiechert structural model to describe the dynamic behaviour of graphene papers, which can be a general model for macroscopic materials of two-dimensional macromolecules. We find that the stress relaxation of MAGMs originates from sheet slippage and wrinkle stretching in laminated structures. We develop an interlayer crosslinking strategy to efficiently depress the stress relaxation of graphene papers. This general model guides us to promote the elasticity of graphene papers by vulcanization, in a close analogy with crosslinking rubbers. In summary, we reveal the important stress relaxation behaviour of graphene materials and present an efficient interlayer crosslinking method to conquer this problem. The general structural model offers a new philosophy to treat graphene materials as classical polymers and allows us to use versatile concepts in the polymer industry to design graphene materials.

Introduction

Stress relaxation, describing the decreasing trend of stress at a given strain of a material along with time, plays a vital role in determining the material's bearing capability to dynamic loading, which possibly causes dangerous mechanical failure in practical applications. Such a phenomenon is particularly common in polymeric materials because of the viscoelastic nature of the constituent macromolecule chains,[1–5] as exemplified in our daily lives by loosening of elastic bands. Therefore, the deep understanding of this dynamic behaviour, especially for newly emerged materials, is a prerequisite before they get widely used.

Graphene building blocks have extraordinary properties, for example, the record mechanical strength (130 GPa of tensile strength and 1.1 TPa of modulus) and excellent electrical and thermal conductivities.[6–8] Great advances have been achieved to translate these attractive merits into MAGMs with high mechanical and functional properties, usually through the ordered assembly method.[9–12] Graphene fibres[13–20] and bucky papers[21–30] with laminated structures are two mechanically

[a] MOE Key Laboratory of Macromolecular Synthesis and Functionalization, Department of Polymer Science and Engineering, Key Laboratory of Adsorption and Separation Materials & Technologies of Zhejiang Province, Zhejiang University, 38 Zheda Road, Hangzhou 310027, P. R. China. E-mail: zhenxu@zju.edu.cn, chaogao@zju.edu.cn

[b] National Key Laboratory of Science and Technology on Advanced Composites in Special Environments, Harbin Institute of Technology, Harbin 150080, P. R. China

† Electronic supplementary information (ESI) available: SEM images, relaxation curves, EDS mapping, XPS spectra and cyclic tests. See DOI: 10.1039/c8mh00817e

strong representatives. Since 2011, the mechanical strength and modulus of wet-spun graphene fibres have leaped to 2.2 GPa and 400 GPa, respectively, by systematically diminishing the multiscale defects of graphene laminated structures.[31] Graphene papers also synchronously exhibited 0.8 GPa of strength and 6.4 GPa of modulus.[32] These static mechanical merits of MAGMs are encouraging more efforts on further improvements and their future uses as structural materials.[33]

Beyond the achievement of high static strength, the dynamic mechanical behaviour of macroscopic graphene materials has long been ignored and only a few reports paid attention to the viscoelastic behaviour and fatigue phenomenon of graphene papers.[34,35] Vinod *et al.*[34] illustrated that graphene oxide (GO) paper shows different mechanical responses to different strain rates due to plastic deformation of the layer sliding under tension. Wan and colleagues[35] revealed a fatigue property in graphene paper and proposed a synergistic effect to restrain this fatigue by introducing polymer binders. However, stress relaxation – an important dynamic behaviour – has never been noticed. This vacancy of comprehension on the stress relaxation could dim the great hope of high performance graphene materials for structural uses.

In this report, we launch the investigation on the stress relaxation of MAGMs. We first observed a fatal stress relaxation of graphene bucky papers. The relaxation behaviour of graphene materials, a typical two-dimensional (2D) macromolecular system, conforms to a Maxwell–Wiechert model as is described in polymeric materials. The interlayer flow between graphene sheets mainly accounts for the stress relaxation. We present an interlayer crosslinking strategy to conquer the stress relaxation of graphene papers, by virtue of either coordination bonds of metal ions or covalent bonds *via* vulcanization. The residual stress of graphene papers scaled with the energy and density of the crosslinking bonds, and was promoted to 84.1% after vulcanization, significantly higher than the 14.7% of GO papers and 43.2% of the original reduced graphene (RG) papers. Moreover, a highly elastic graphene paper with a large 10% strain was designed through depressing the relaxation trend, analogous to using vulcanization to produce polymeric elastic rubber. Our work unveils the stress relaxation issue of MAGMs and offers a crosslinking strategy to conquer it effectively. Deeper understanding on the relaxation is essential for the further design and fabrication of graphene materials with well-rounded mechanical performances, paving the way for their realistic applications as structural components.

Results and discussion

We prepared GO papers by blade casting its aqueous dispersion, a prevailing method to fabricate GO papers.[26] The moving blade guided the alignment of the GO sheets and the evaporation of water compressed the GO sheets to assemble into a laminated structure accompanied with randomly spreading wrinkles (Fig. S1, ESI†). The subsequent chemical reduction by hydroiodic acid solution was conducted to turn GO papers to RG papers (detailed procedures are described in the Experimental section), which not only eliminated the oxygen-containing functional groups but also brought about a thinner thickness from 5.2 μm of GO paper to 3.0 μm of RG paper (Fig. S2, ESI†). After reduction, RG papers became hydrophobic as compared with the highly hydrophilic GO papers. We picked GO and RG papers as models to analyze the mechanical behaviour of graphene laminated materials.

The uniaxial tensile curves of GO and RG papers show their mechanical strength, and importantly, reveal their viscoelastic behaviour under tension (Fig. 1A). GO papers exhibited a lower strength (56 MPa) but a higher breakage elongation (2.82%) as

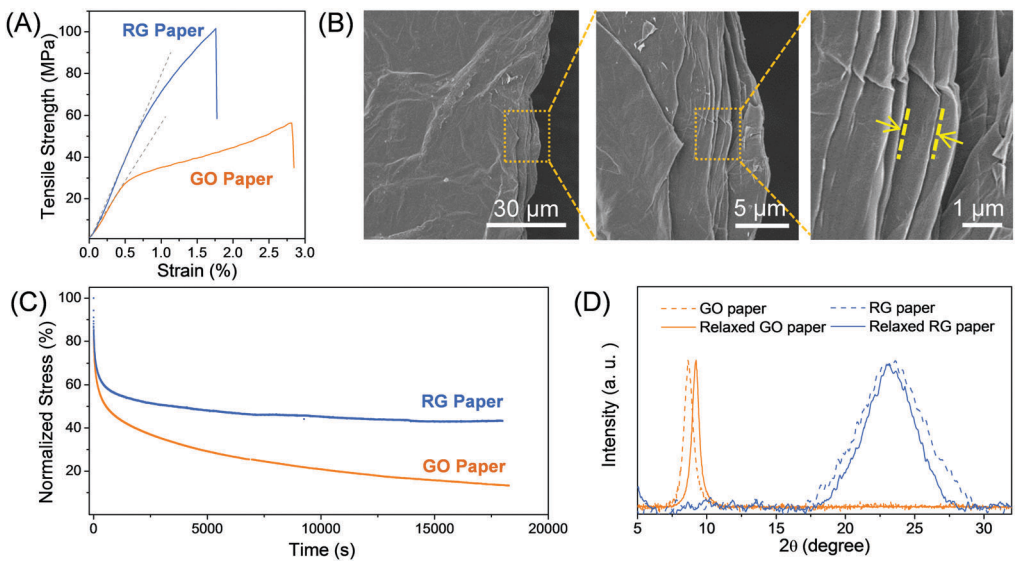

Fig. 1 Viscoelastic mechanical behaviours of GO and RG papers. (A) Stress–strain curves of GO and RG cast papers. The dotted lines indicate the elastic regions of each paper. (B) SEM images of fracture tips exhibiting slipping bands. (C) Stress relaxation behaviour of GO and RG papers at a strain of 1.2%. (D) XRD spectra of GO and RG papers before (dashed line) and after (solid line) relaxation.

compared with RG papers (102 MPa at 1.70%), which are the average values from previous reports.[25,36,37] The nonlinear shape of the tensile curves excludes pure elastic behaviour and reveals a plastic behaviour, that is, the increasing of stress becomes slower as the strain proceeds.[34,37,38] GO paper exhibited a nearly ideal elastic response (16% of the breakage elongation) before 0.45% strain and proceeded to a plastic region until breakage; while RG paper had a wider elastic region before 0.74%, around 43% of the breakage elongation. By investigating the fracture surface of GO papers *via* scanning electron microscopy (SEM), the plastic deformation can be attributed to the flow between constituent GO sheets (the slipping bands with a width of 1–3 μm), possibly accompanied by the stretching of wrinkles (Fig. 1B). This viscous slippage between GO sheets also explained the previous observation that the breakage elongation of GO papers was closely related to strain rates.[34]

The viscoelasticity implies the occurrence of stress relaxation, as demonstrated in polymers.[1–5] To confirm this, we examined the GO and RG papers and found severe stress relaxation behaviour (Fig. 1C). When maintaining a certain strain at 1.2%, GO and RG papers went through a decreasing stress, and remained at 14.7% and 43.2% of their initial stresses, respectively, after only 18 000 s. This means that not only GO but also RG papers would lose capability under loading after several hours, although they exhibited high mechanical tensile strength. The remaining stress ratios after relaxation are close to the percentage of elastic strain in both GO (16%) and RG (43%) papers, indicating the elastic region of graphene papers can be maintained from relaxation. The weaker stress kept in GO papers matches its longer plastic region in tensile tests (Fig. 1A), implying that the viscous flow between laminated GO sheets is the same structural reason for the plasticity and relaxation behaviour. We also tracked the structural evolution brought by relaxation through X-ray diffraction (XRD). After relaxation, the interlayer spacing of GO papers became narrower, as shown by the shift of diffraction peak from 8.59° to 9.19°. At the same time, the sharpened diffraction peaks in relaxed GO and RG papers denote a higher regularity of laminated structure, which results from the reorientation of constituent GO and RG sheets during relaxation (Fig. 1D).[39,40] Hydrogen bonds and van der Waals attractions between interlayers are the dominant forces and from these two weak dynamic bonds it is hard to immobilize constituent sheets together, therefore giving rise to the easy interlayer slippage and relaxation.[41,42] We also found that higher strain caused less relaxation retention (Fig. S3, ESI†). For example, GO papers maintained 49.2% of their initial stress after relaxation at 0.4% strain while they kept only 17.4% at 2.0% strain. RG papers withstood 55.1% stress at 0.4% strain, larger than that (43.2%) in the case of 1.2% strain.

Stress relaxation is a universal dynamic behaviour in varied graphene laminated papers, including filtrated GO and RG papers[25] and cast papers of small size GO (named as SGO and RSG papers, respectively), as shown in Fig. S4 and S5, ESI.† Compared with GO and RG papers by blade casting, filtrated GO and RG papers showed higher residual stress (about 35.1% and 51.4% remained, respectively), due to their tight stacking structures (XRD patterns in Fig. S4, ESI†).

The viscoelastic behaviour, typically for polymers, can be generally described by the Maxwell model that consists of the combination of elastic spring and viscous dashpot units.[1–3] The simple stress relaxation behaviour of a single Maxwell model can be expressed as

$$\sigma(t) = \sigma_0 e^{-t/\tau} \quad (1)$$

where σ_0 is initial stress at the beginning of relaxation and τ is characteristic relaxation time related to the elastic modulus of spring (E) and the intrinsic viscosity (η) of dashpot.

By data fitting, the GO and RG paper systems deviated from this simple Maxwell model (Fig. S6, ESI†).[1–3] Considering the multilevel structure of graphene laminates, we proposed a ternary Maxwell–Wiechert model which encompasses an independent spring to describe the residual stress and two parallel Maxwell series units (Scheme 1).[43,44] This ternary model fits the stress relaxation curves of GO and RG papers with high accuracy with an adjusted coefficient of determination over 0.99 (Table S1, ESI†). In this modified model, stress–time curves during stress relaxation can be expressed by the following equation:

$$\sigma(t) = \sigma_\infty + \sigma_1 e^{-t/\tau_1} + \sigma_2 e^{-t/\tau_2} \quad (2)$$

where σ_∞ is residual stress for the standalone spring. σ_1 and σ_2, and τ_1 and τ_2 are the initial stresses and characteristic relaxation times of each Maxwell unit. To distinguish two Maxwell units, we ruled that $\tau_1 < \tau_2$.

For convenience of comparison, eqn (2) is divided by σ_0 to get the normalized stress:

$$A(t) = A_\infty + A_1 e^{-t/\tau_1} + A_2 e^{-t/\tau_2} \quad (3)$$

A_∞, A_1 and A_2 represent $\sigma_\infty/\sigma_0 \times 100\%$, $\sigma_1/\sigma_0 \times 100\%$ and $\sigma_2/\sigma_0 \times 100\%$, respectively.

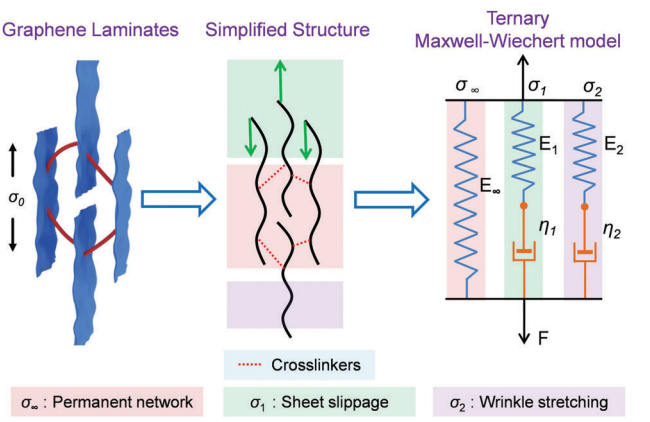

Scheme 1 The structural projection of the ternary Maxwell–Wiechert model of graphene laminated structure. It includes one independent spring and two parallel simple Maxwell units, which can be directed to the permanent network, the sheet slippage and the wrinkle stretching, respectively.

We projected this model to multilevel structures of graphene laminates, as demonstrated in Scheme 1. A_∞ denotes the graphene piled network with high enough strength to resist the slippage and relaxation, similar to the crosslinking network of polymeric rubbers. A_1 and A_2 represent the laminates that are easy to flow and the possible wrinkles that can be stretched, respectively. Notably, these two parts can be immobilized to form permanent networks by enhancing the interlayer attraction. The model predicts that a larger strain can accelerate the viscous slippage between RG sheets, generating faster relaxation of RG laminates, which is consistent with experimental results (Fig. S3 and Table S1, ESI†).

From the model, it is concluded that the viscous flow of constituent sheets determines the stress relaxation. Therefore, enhancing interlayer attraction should be feasible to retard sheet slippage and prevent stress relaxation. The rich oxygen functional groups and the disordered conjugated domains on the GO and RG sheets enable facile crosslinking by either coordination bonds between metal ions and oxygen groups[15,22,45] or interlayer covalent bonds from isolated carbon double bonds.[38,46] Hence, we proposed a crosslinking strategy to relieve the severe mechanical relaxation of graphene laminated materials. Metal ions with different charges and sulphur as crosslinkers with ascending bonding energies were chosen to enhance the interlayer attraction.

The relaxation curves distinctively exhibited the trend that the relaxation of RG papers was retarded by introducing crosslinkers (Fig. 2A). The maintained stress ratio increased with the raised bonding energy in a sequence from divalent ions to trivalent ions and covalent carbon–sulphur bonds. The relaxation behaviour of all the crosslinked RG papers still conformed to our proposed model for pristine GO and RG papers (Fig. S7, ESI†). In the frame of the ternary model (eqn (3)), the divalent ions (Ca^{2+} and Mg^{2+}) promoted the residual stress (A_∞) of RG papers (RG-Ca and RG-Mg, respectively) to 49.6% and 50.8% after 18 000 s, respectively, higher than that of GO papers (14.7%) and that of pristine RG papers (43.2%). For trivalent Fe^{3+} ions (0.45 at%), A_∞ of crosslinked RG papers (RG-Fe) increased to an even higher value of 58.9%, attributed to the stronger electrostatic interactions and coordination bonding of highly charged transition metal ions to the oxygen functional groups.[22,45] As for the covalently crosslinked RG paper by sulphur (RG-S), A_∞ was improved to 84.1%, nearly 95% higher than that of pristine RG papers. The considerably improved capability to resist relaxation is because C–S covalent links can bind RG sheets together to prevent viscous slippage. Energy dispersive spectroscopy (EDS) mapping of the section (Fig. 2E) confirms the homogenous existence of sulphur inside and the X-ray photoelectron spectroscopy (XPS) further proves that sulphur exists as a form of C–S bonding (Fig. S8, ESI†). In crosslinked RG papers, the increasing of A_∞ accompanied with the decreasing of viscous parts (A_1 and A_2), implies that the mutable structure of RG papers can be changed to mechanically stable networks by chemical engineering (Fig. 2B). Besides, the invariance of relaxation time (τ_1 and τ_2) of pristine RG and crosslinked RG papers illustrates that the remaining relaxation part was generally dominated by the same kinetic molecular interactions (Fig. 2C). This means that interlayer transient networks in un-crosslinked parts have a similar bond lifetime, which determines the alike plastic deformation under stress (dashpot units in the model). The crosslinking strategy also brings an increase in Young's modulus of RG papers (from 5.4 GPa of pristine RG paper to 7.2 GPa of crosslinked RG papers) due to strong interlayer interactions (Fig. S9, ESI†). Moreover, RG and crosslinked RG papers show good thermal conductivities around 45–65 W m^{-1} K^{-1}, close to the metal stannum (Fig. S10 and Table S2, ESI†). For RG-S paper, the increase of thermal conductivity is mainly due to the reduction

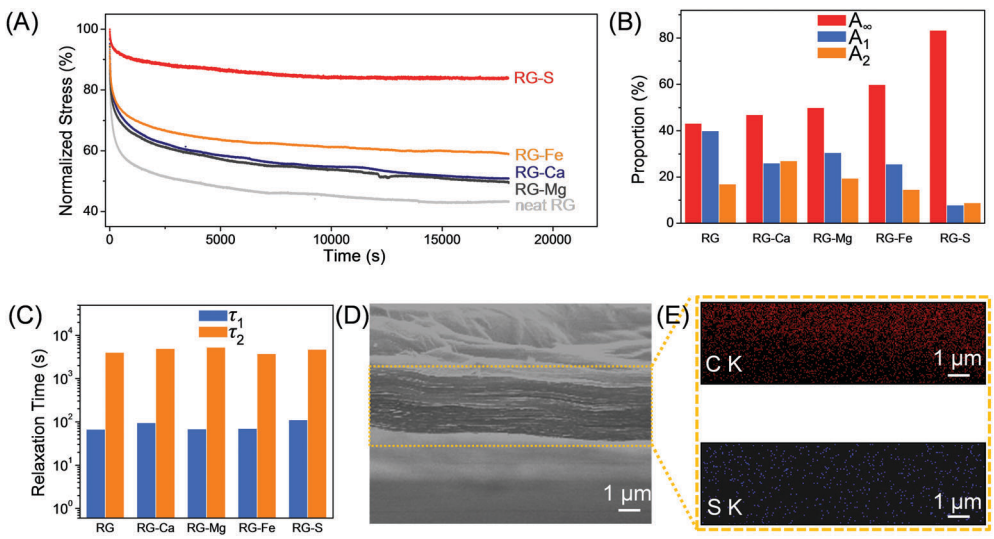

Fig. 2 Crosslinking strategy to restrain relaxation. (A) Stress relaxation curves of crosslinked RG papers at a strain of 1.2%. Curve fitting results of these papers based on eqn (3) are shown in (B) proportions of each unit and (C) the corresponding characteristic relaxation time (τ). (D) SEM images of sections and (E) the corresponding EDS mapping of vulcanized RG paper.

of RG sheets by high temperature during the vulcanization process.[25]

The crosslinking between RG sheets to prevent their viscous slippage – the structural root for stress relaxation – is seen in the micro morphology of fracture surfaces (Fig. 3). As A_∞ was improved, the slippage between RG sheets was depressed, indicating that the distinct step fracture morphology evolved into a smooth fracture surface (Fig. 3A–C). For pristine RG papers, the fracture lines were rough curves and the average width of slipping bands was measured as 1.1 μm, narrower than 1.8 μm in GO papers, but much longer than the 0.5 μm of Mg^{2+} and vulcanized RG papers (Fig. 3D). The narrowing of slipping bands demonstrates the principle that crosslinking can impede viscous flow between graphene sheets and thus prevent the stress relaxation (Fig. 3E).

The crosslinking density can also control the stress relaxation behaviour, besides the type of crosslinking bond. We chose Fe^{3+} crosslinked RG paper as the typical system (Fig. 4). As the Fe^{3+} concentration increased, A_∞ ranged from 45.3% to 63.7%, heading to a 47.4% increase compared with neat RG paper (Fig. 4A). A_∞ showed a nearly monotonous increase with the increase of Fe^{3+} atomic content below 0.9% (Fig. 4B). EDS mapping on paper section surfaces revealed homogenous distribution of Fe^{3+} inside the interlayer gallery (Fig. 4C, Fig. 4D and Fig. S11, ESI†). Accompanying the increase of A_∞, the viscous parts (A_1 and A_2) were gradually transformed into elastic parts by increasing the ion crosslinking density. Additionally, Fe^{3+} crosslinked RG papers still have unvaried relaxation times (τ_1 and τ_2), which implies that the relaxation still follows the same kinetic mechanism (Fig. S12 and Table S1, ESI†).

This ternary model we have proposed can guide the modulation of the dynamic mechanical properties of MAGMs.

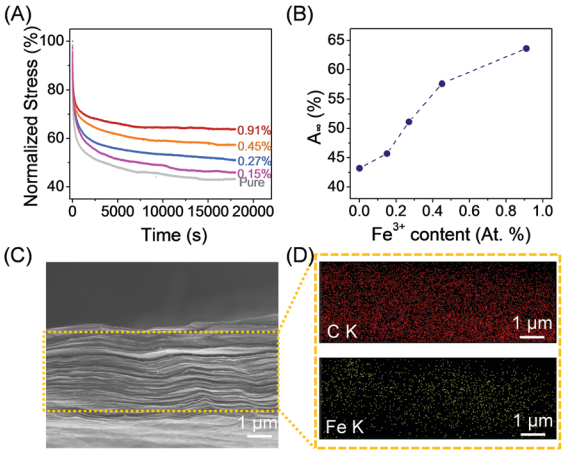

Fig. 4 Stress relaxation behaviour under the influence of crosslinking density in RG papers. (A) Stress relaxation curves of crosslinked RG papers with increasing Fe^{3+} concentration. (B) Normalized equilibrium stress (A_∞) as a function of Fe^{3+} concentration. (C) SEM image of sections and (D) the corresponding EDS mapping of Fe^{3+} crosslinked RG papers with 0.45 at% Fe^{3+}.

We deduced that the interlayer crosslinking can turn the viscous structure to an elastic network, thus enhancing the elasticity of graphene materials, analogous to commercial rubbers, where the chemical crosslinking turns the viscous crude matrix to elastic rubbers, such as vulcanization in polyisoprene and crosslinking reagents in silicon rubber.[1,43,44] Accordingly, starting from our previous collapsed RG papers,[47] we used the vulcanization method to fabricate highly elastic graphene papers with high breakage elongation. Sulphur radicals generated by heating sulphur can initiate the radical addition reaction with isolated carbon double bonds in RG sheets and

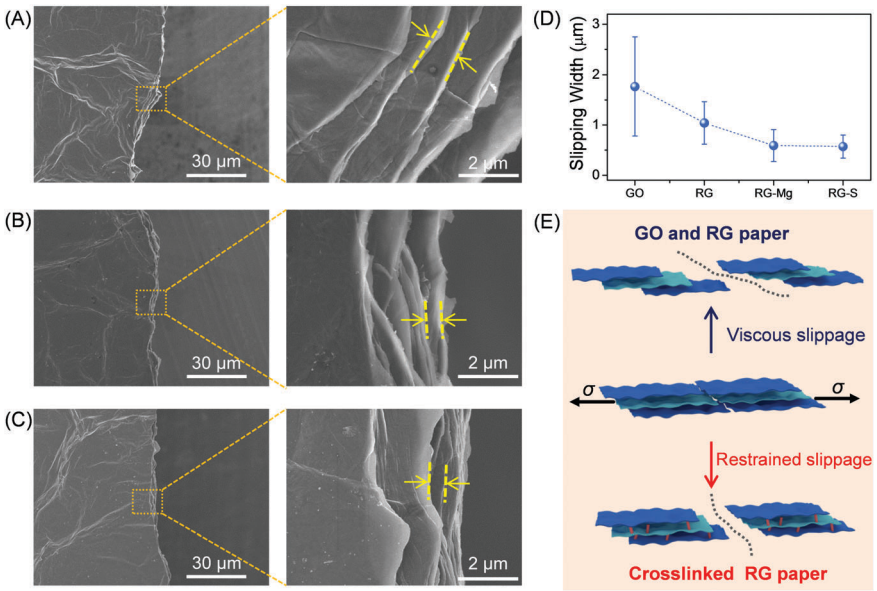

Fig. 3 Interlayer slippage behaviour restrained by interlayer crosslinking. SEM images of fracture tips of (A) RG, (B) RG-Mg and (C) RG-S papers. (D) Statistics results of slipping band widths of GO, RG and crosslinked RG papers. Error bars represent the standard deviation of band width. (E) Schematic sketch of fracture differences between viscous slippage of graphene sheets in GO and RG papers and restrained slippage in crosslinked graphene papers.

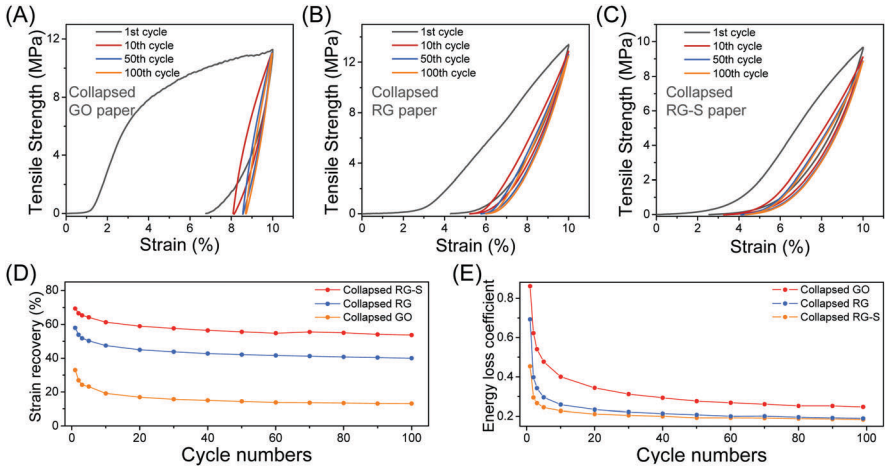

Fig. 5 Elastic graphene papers by vulcanization. Cyclic tensile tests of collapsed (A) GO, (B) RG and (C) RG-S papers at a strain of 10% for 100 cycles. (D) Strain recovery and (E) energy loss coefficients of these three papers.

form interlayer covalent bonds, as in the case of polyisoprene rubbers.[48,49] The vulcanized collapsed RG paper remained at 76.4% stress after relaxation at 10% strain (Fig. S13, ESI†), which is better than that of pristine collapsed GO and RG papers (50.2% and 59.6% stress remaining, respectively). This result suggests that crosslinking networks through vulcanization can indeed make graphene laminates more elastic by retarding sheet slippage. In cyclic tensile tests at 10% strain with a rate of 2 mm min^{-1}, the vulcanized papers showed a wider elastic deformation strain range (from 2% to 9% strain), less plastic deformation (2%) and smaller hysteresis during cyclic tests (Fig. 5C). As a comparison, collapsed GO and RG papers (Fig. 5A and B) possessed narrower elastic ranges (1% and 3%) and higher plastic deformations (8% and 6%). The vulcanization brought a considerably improved strain recovery to 55%, higher than 40% for RG papers and 15% for GO papers (Fig. 5D). At the same time, the minimum energy loss coefficient was decreased to 0.18 (Fig. 5E), as another proof of the enhanced elasticity. At varied strains (5% and 15%) and strain rates (1 and 5 mm min^{-1}), vulcanized RG papers exhibited the highest strain recovery and lowest energy loss coefficients as compared with pristine collapsed RG papers without crosslinking (Fig. S14 and S15, ESI†). Importantly, the strain recovery scaled with the strain rate, increasing from 48% at 1 mm min^{-1} to 57% at 5 mm min^{-1} (Fig. S16, ESI†). This trend is possibly attributed to the plastic movement between RG sheets at low strain rates, which causes higher energy dissipation, resembling the rate-dependent mechanical behaviour of polymers.[50]

Conclusion

In summary, we launched a systematic investigation of the stress relaxation problem of MAGMs. For the first time, we observed the severe stress relaxation behaviour of GO and RG papers with laminated structures. Our results revealed that interlayer viscous slippage between graphene sheets mainly accounts for the stress relaxation and viscoelastic behaviour. A ternary Maxwell–Wiechert model was proposed to generally describe the stress relaxation behaviour of MAGMs. We also offered an efficient interlayer crosslinking method to depress the stress relaxation. The dynamic behaviour of macroscopic graphene materials can be well controlled by the bonding energy together with the bonding density. The interlayer crosslinking strategy was also used to improve the elasticity of graphene papers with high breakage elongation. Our work uncovers an important dynamic mechanical behaviour of MAGMs and the proposed interlayer crosslinking method directs the fabrication of graphene materials with qualified dynamic properties for realistic structural applications. The ternary Maxwell–Wiechert model we developed should become a general model for macroscopic materials of 2D macromolecules, which will be very useful to deepen the understanding of the static and dynamic behaviour of macroscopically assembled materials of graphene and other 2D nanomaterials.

Experimental section

Fabrication of GO and RG papers

An aqueous GO dispersion was purchased from Hangzhou Gaoxi Technology Co. Ltd (www.gaoxitech.com). The typical GO sheet size was about 30–100 μm through SEM inspection and the size of SGO was about 5–20 μm (Fig. S17, ESI†). A GO dispersion of 6 mg mL^{-1} was first degassed using a conditioning mixer for 5 min and then was cast onto a PET substrate with a thickness of 2 mm and scraped with blade. After drying at room temperature for 24 h, free-standing paper was torn off from the substrate for further drying under vacuum at 80 °C for 4 h to obtain GO paper. To obtain RG paper, GO paper was reduced in a mixture solution with hydroiodic acid (HI, 50 wt%) and ethanol (v/v = 1 : 3) for 24 h at 60 °C. After washing with ethanol three times to remove residual HI and I_2, the RG paper was dried under vacuum at 90 °C for 12 h.

Fabrication of crosslinked RG papers

For ion-crosslinked RG papers, RG papers were immersed in an ethanol/water (v/v = 5 : 1) solution with 0.1 M $FeCl_3$, $MgCl_2$ or $CaCl_2$ for 30 min, respectively. Then, these papers were washed with ethanol to remove the rest of the salt on the paper surface and dried under vacuum at 90 °C for 12 h. Different concentrations of Fe^{3+} crosslinked RG papers were made by changing the $FeCl_3$ concentration from 0.01 M to 0.5 M in the ethanol/water (v/v = 5 : 1) solution. For vulcanization, RG paper was first immersed in a carbon disulphide solution with saturated sulphur for 30 min and dried at room temperature for 24 h. Then, the paper was treated in a N_2 atmosphere at 180 °C for 30 min to obtain vulcanized RG paper.

Fabrication of filtrated graphene papers

A GO dispersion (4 mg mL^{-1}) was first degassed using a conditioning mixer for 5 min, then filtered onto a cellulose filter membrane with an average pore size of 0.22 μm for 72 h. After filtration, the as-prepared paper was dried under vacuum at 80 °C for 4 h to finally obtain filtrated GO paper. The reduction process was the same as that for the cast RG papers.

Fabrication of collapsed graphene papers

The method to make collapsed graphene paper was published in our previous work.[47] Typically, the aqueous GO dispersion was first replaced with DMF *via* centrifugation washing three times. The obtained dispersion was cast onto PTFE substrate and then immersed in ethyl acetate for 6 h. After drying in air at 70 °C for 6 h, we obtained collapsed GO paper. To achieve collapsed RG and vulcanized-RG paper, the same method was used as that to treat the GO paper above.

Characterization

SEM images were taken on Hitachi S4800 field emission system. X-ray diffraction data was collected on a Philips X'Pert PRO diffractometer using Cu Kα1 radiation (40 kV, 40 mA) with a ray wavelength (λ) of 1.5418 Å. XPS was performed using a PHI 5000C ESCA System operated at 14.0 kV and all binding energies were referenced to the C 1s neutral carbon peak at 284.8 eV. All mechanical tests were performed on a microcomputer control electronic universal testing machine (RGWT-400-20, REGER). Tensile testing was performed by stretching a slip of paper at a rate of 1 mm min^{-1}. Stress relaxation testing was performed by stretching a slip to a certain strain at a rate of 1 mm min^{-1}, followed by maintaing the strain to record the evolved stress along with time. Cyclic tensile tests were performed by stretching a strip of paper to a certain strain (5%, 10% and 15%) at rates of 1, 2 or 5 mm min^{-1}. The typical size of a strip for mechanical testing was 10 mm × 2 mm. Thermal conductivity was measured by the steady-state electro-thermal technique,[51] in which temperature profiles were collected by a FLIR T630sc infrared camera with a close-up lens.

Conflicts of interest

There are no conflicts to declare.

Acknowledgements

This work is supported by the National Natural Science Foundation of China (No. 21325417, 51533008, 51703194 and 51603183), National Key R&D Program of China (No. 2016YFA0200200), Hundred Talents Program of Zhejiang University (188020*194231701/113) and Fundamental Research Funds for the Central Universities (2017QNA4036 and 2018QNA4058).

Notes and references

1 A. V. Tobolsky, *J. Appl. Phys.*, 1956, **27**, 673–685.
2 A. N. Gent, *J. Appl. Polym. Sci.*, 1962, **6**, 433–441.
3 C. Ortiz, C. K. Ober and E. J. Kramer, *Polymer*, 1998, **39**, 3713–3718.
4 V. K. Kothari, R. Rajkhowa and V. B. Gupta, *J. Appl. Polym. Sci.*, 2001, **82**, 1147–1154.
5 L. Imbernon, S. Norvez and L. Leibler, *Macromolecules*, 2016, **49**, 2172–2178.
6 Z. Li, Z. Liu, H. Sun and C. Gao, *Chem. Rev.*, 2015, **115**, 7046–7117.
7 K. S. Novoselov, A. K. Geim, S. V. Morozov, D. Jiang, Y. Zhang, S. V. Dubonos, I. V. Grigorieva and A. A. Firsov, *Science*, 2004, **306**, 666–669.
8 C. Lee, X. Wei, J. W. Kysar and J. Hone, *Science*, 2008, **321**, 385–388.
9 Z. Xu and C. Gao, *ACS Nano*, 2011, **5**, 2908–2915.
10 Z. Xu, L. Peng, Y. Liu, Z. Liu, H. Sun, W. Gao and C. Gao, *Chem. Mater.*, 2016, **29**, 319–330.
11 L. Kou, Y. Liu, C. Zhang, L. Shao, Z. Tian, Z. Deng and C. Gao, *Nano-Micro Lett.*, 2017, **9**, 51.
12 R. Narayan, J. E. Kim, J. Y. Kim, K. E. Lee and S. O. Kim, *Adv. Mater.*, 2016, **28**, 3045–3068.
13 Z. Xu and C. Gao, *Nat. Commun.*, 2011, **2**, 571.
14 Z. Xu and C. Gao, *Acc. Chem. Res.*, 2014, **47**, 1267–1276.
15 Z. Xu, H. Sun, X. Zhao and C. Gao, *Adv. Mater.*, 2013, **25**, 188–193.
16 M. K. Shin, B. Lee, S. H. Kim, J. A. Lee, G. M. Spinks, S. Gambhir, G. G. Wallace, M. E. Kozlov, R. H. Baughman and S. J. Kim, *Nat. Commun.*, 2012, **3**, 650.
17 Z. Xu and C. Gao, *ACS Nano*, 2012, **6**, 7103–7113.
18 G. Xin, T. Yao, H. Sun, S. M. Scott, D. Shao, G. Wang and J. Lian, *Science*, 2015, **349**, 1083–1087.
19 Y. Liu, Z. Xu, J. Zhan, P. Li and C. Gao, *Adv. Mater.*, 2016, **28**, 7941–7947.
20 Y. Liu, Z. Xu, W. Gao, Z. Cheng and C. Gao, *Adv. Mater.*, 2017, **29**, 1606794.
21 M. Zhang, Y. Wang, L. Huang, Z. Xu, C. Li and G. Shi, *Adv. Mater.*, 2015, **27**, 6708–6713.
22 C. N. Yeh, K. Raidongia, J. Shao, Q. H. Yang and J. Huang, *Nat. Chem.*, 2014, **7**, 166–170.
23 Z. Liu, Z. Li, Z. Xu, Z. Xia, X. Hu, L. Kou, L. Peng, Y. Wei and C. Gao, *Chem. Mater.*, 2014, **26**, 6786–6795.
24 B. Shen, W. Zhai and W. Zheng, *Adv. Funct. Mater.*, 2014, **24**, 4542–4548.

25 H. Chen, M. B. Müller, K. J. Gilmore, G. G. Wallace and D. Li, *Adv. Mater.*, 2008, **20**, 3557–3561.
26 L. Peng, Z. Xu, Z. Liu, Y. Guo, P. Li and C. Gao, *Adv. Mater.*, 2017, **29**, 1700589.
27 J. Peng and Q. Cheng, *Adv. Mater.*, 2017, **29**, 1702959.
28 Y. Tian, Y. Cao, Y. Wang, W. Yang and J. Feng, *Adv. Mater.*, 2013, **25**, 2980–2983.
29 E. Zhou, J. Xi, Z. Xu, Y. Guo, L. Peng, W. Gao, J. Ying, Z. Chen and C. Gao, *Nanoscale*, 2017, **9**, 18613–18618.
30 E. Zhou, J. Xi, Y. Guo, Y. Liu, Z. Xu, L. Peng, W. Gao, J. Ying, Z. Chen and C. Gao, *Carbon*, 2018, **133**, 316–322.
31 Z. Xu, Y. Liu, X. Zhao, L. Peng, H. Sun, Y. Xu, X. Ren, C. Jin, P. Xu, M. Wang and C. Gao, *Adv. Mater.*, 2016, **28**, 6449–6456.
32 Y. Wen, M. Wu, M. Zhang, C. Li and G. Shi, *Adv. Mater.*, 2017, **29**, 1702831.
33 Z. Xu and C. Gao, *Mater. Today*, 2015, **18**, 480–492.
34 S. Vinod, C. S. Tiwary, L. D. Machado, S. Ozden, J. Cho, P. Shaw, R. Vajtai, D. S. Galvao and P. M. Ajayan, *Nano Lett.*, 2016, **16**, 1127–1131.
35 S. Wan, Q. Zhang, X. Zhou, D. Li, B. Ji, L. Jiang and Q. Cheng, *ACS Nano*, 2017, **11**, 7074–7083.
36 L. Zhang, N. T. Alvarez, M. Zhang, M. Haase, R. Malik, D. Mast and V. Shanov, *Carbon*, 2015, **82**, 353–359.
37 D. A. Dikin, S. Stankovich, E. J. Zimney, R. D. Piner, G. H. Dommett, G. Evmenenko, S. T. Nguyen and R. S. Ruoff, *Nature*, 2007, **448**, 457–460.
38 Y. Gao, L. Q. Liu, S. Z. Zu, K. Peng, D. Zhou, B. H. Han and Z. Zhang, *ACS Nano*, 2011, **5**, 2134–2141.
39 W. Tie, S. S. Bhattacharyya, Y. J. Lim, S. W. Lee, T. H. Lee, Y. H. Lee and S. H. Lee, *Opt. Express*, 2013, **21**, 19867–19879.
40 Z. Dai, Y. Wang, L. Liu, X. Liu, P. Tan, Z. Xu, J. Kuang, Q. Liu, J. Lou and Z. Zhang, *Adv. Funct. Mater.*, 2016, **26**, 7003–7010.
41 Y. Liu, B. Xie, Z. Zhang, Q. Zheng and Z. Xu, *J. Mech. Phys. Solids*, 2011, **60**, 591–605.
42 N. V. Medhekar, A. Ramasubramaniam, R. S. Ruoff and V. B. Shenoy, *ACS Nano*, 2010, **4**, 2300–2306.
43 E. B. D. da Rocha, F. N. Linhares, C. F. S. Gabriel, A. M. F. de Sousa and C. R. G. Furtado, *Appl. Clay Sci.*, 2018, **151**, 181–188.
44 H. J. Maria, N. Lyczko, A. Nzihou, K. Joseph, C. Mathew and S. Thomas, *Appl. Clay Sci.*, 2014, **87**, 120–128.
45 S. Park, K. S. Lee, G. Bozoklu, W. Cai, S. T. Nguyen and R. S. Ruoff, *ACS Nano*, 2008, **2**, 572–578.
46 C. Gianfranco, R. Valentina, D. N. Sergio and L. Nicolais, *Nanoscale Res. Lett.*, 2013, **8**, 94.
47 Y. Xiao, Z. Xu, Y. Liu, L. Peng, J. Xi, B. Fang, F. Guo, P. Li and C. Gao, *ACS Nano*, 2017, **11**, 8092–8102.
48 R. Ding and A. I. Leonov, *J. Appl. Polym. Sci.*, 1996, **61**, 455–463.
49 A. P. Susamma, V. T. E. Mini and A. P. Kuriakose, *J. Appl. Polym. Sci.*, 2001, **79**, 1–8.
50 M. C. Boyce and A. D. Mulliken, *Int. J. Solids Struct.*, 2006, **43**, 1331–1356.
51 Y. Yue, G. Eres, X. Wang and L. Guo, *Appl. Phys. A: Mater. Sci. Process.*, 2009, **97**, 19–23.

